

# Accurate Diagnosis of SARS-CoV-2 JN.1 by Sanger Sequencing of Receptor-Binding Domain Is Needed for Clinical Evaluation of Its Immune Evasion

Sin Hang Lee

Milford Molecular Diagnostics Laboratory, Milford, CT, USA

Email: shlee01@snet.net

**How to cite this paper:** Lee, S.H. (2024) Accurate Diagnosis of SARS-CoV-2 JN.1 by Sanger Sequencing of Receptor-Binding Domain Is Needed for Clinical Evaluation of Its Immune Evasion. *Journal of Biosciences and Medicines*, 12, 69-78.  
<https://doi.org/10.4236/jbm.2024.124007>

**Received:** March 13, 2024

**Accepted:** April 7, 2024

**Published:** April 10, 2024

Copyright © 2024 by author(s) and Scientific Research Publishing Inc. This work is licensed under the Creative Commons Attribution International License (CC BY 4.0).

<http://creativecommons.org/licenses/by/4.0/>



Open Access

## Abstract

**Background:** Omicron JN.1 has become the dominant SARS-CoV-2 variant in recent months. JN.1 has the highest number of amino acid mutations in its receptor binding domain (RBD) and has acquired a hallmark L455S mutation. The immune evasion capability of JN.1 is a subject of scientific investigation. The US CDC used SGTF of TaqPath COVID-19 Combo Kit RT-qPCR as proxy indicator of JN.1 infections for evaluation of the effectiveness of updated monovalent XBB.1.5 COVID-19 vaccines against JN.1 and recommended that all persons aged  $\geq 6$  months should receive an updated COVID-19 vaccine dose. **Objective:** Recommend Sanger sequencing instead of proxy indicator to diagnose JN.1 infections to generate the data based on which guidelines are made to direct vaccination policies. **Methods:** The RNA in nasopharyngeal swab specimens from patients with clinical respiratory infection was subjected to nested RT-PCR, targeting a 398-base segment of the N-gene and a 445-base segment of the RBD of SARS-CoV-2 for amplification. The nested PCR amplicons were sequenced. The DNA sequences were analyzed for amino acid mutations. **Results:** The N-gene sequence showed R203K, G204R and Q229K, the 3 mutations associated with Omicron BA.2.86 (+JN.1). The RBD sequence showed 24 of the 26 known amino acid mutations, including the hallmark L455S mutation for JN.1 and the V483del for BA.2.86 lineage. **Conclusions:** Sanger sequencing of a 445-base segment of the SARS-CoV-2 RBD is useful for accurate determination of emerging variants. The CDC may consider using Sanger sequencing of the RBD to diagnose JN.1 infections for statistical analysis in making vaccination policies.

## Keywords

Omicron JN.1, SARS-CoV-2, Sanger Sequencing, RBD, L455S Mutation, Immune Evasion, Vaccination Policies, CDC

---

## 1. Introduction

As SARS-CoV-2 is allowed to spread among human populations, genetic changes occur and accumulate in the circulating virus, resulting in numerous variants since July, 2020. The newly dominant Omicron JN.1 variant has 26 amino acid mutations in its Spike protein ACE2 receptor binding domain (RBD) [1]. According to an estimate made by the Centers for Disease Control and Prevention (CDC) on March 2, 2024 more than 92% of the SARS-CoV-2 isolates were those of the JN.1 variant [2], rising from <0.1% at the end of October 2023 in the United States [3]. Such a rapid takeover by a newly introduced variant among a highly COVID-19 vaccinated population suggested that the JN.1 variant may be a highly immune-evading variant compared with other Omicron variants. However, based on one serum neutralization study conducted in September 2023 in Germany, the JN.1 variant was not associated with further reduced serological protection beyond prior Omicron variants [4]. On the other hand, more recent studies based on breakthrough infections have shown that JN.1 displayed significantly enhanced immune escape and suggested that JN.1 is one of the most immune-evading variants to date due to its acquisition of L455S mutation in the RBD [5] [6].

Recently, CDC's Advisory Committee on Immunization Practices analyzed a group of tests performed at two pharmacy chains on COVID-19 patients 60 - 119 days after receiving updated monovalent XBB.1.5 COVID-19 vaccines, using the reverse transcription-qPCR TaqPath COVID-19 Combo Kit (Thermo Fisher Scientific) as the testing method to define JN.1 infection [7]. The results showed that 49% (95% CI = 19% - 68%) of the 679 positive tests exhibited S-gene target failure (SGTF) as the proxy indicator of JN.1 infection, and 60% (95% CI = 35% - 75%) of the positive tests exhibited S-gene target presence (SGTP) as the proxy indicator of non-JN.1 infection, suggesting that there is substantial vaccine effectiveness against JN.1. Based on these data, the CDC recommended that all persons aged  $\geq 6$  months should receive an updated COVID-19 vaccine dose. However, SGTF is a poor proxy for 69 - 70 del [8] in the N-terminal domain of the S-gene of SARS-CoV-2, which may be unrelated to amino acid mutations in the RBD. Using the latter proxy as the proxy indicator of JN.1 is a highly imprecise approach to diagnose JN.1 because other non-JN.1 variants, such as the variants Alpha, Omicron BA.1, BA.4 and BA.5 as well as BA.2.86, the precursor of JN.1, that have circulated in the U. S. populations, also harbor 69 - 70 del [1].

This paper recommends that Sanger sequencing of a segment of the S-gene RBD [9] [10] of JN.1 be used to verify the variant before each case is accepted as true JN.1 infection for statistics to generate the data based on which guidelines are made to direct vaccination policies and clinical practice.

## 2. Methods

The method used in this report was a diagnostic test formally referred to as “Partial N gene Sanger sequencing for detection of SARS-CoV-2 with reflex S gene mutation screening” developed in Milford Molecular Diagnostics Laboratory under the Connecticut Department of Public Health License CL-0699 and the test is also approved under the Clinical Laboratory Improvement Amendments (CLIA) of 1988 for testing human specimens.

### 2.1. Patient Specimens

Nasopharyngeal swab specimens from patients with clinical respiratory infections were collected by healthcare providers in the month of February 2024. The swabs were immersed in virus transport media or phosphate-buffered saline after collection and sent to the testing laboratory within 48 hours. The specimens were stored at  $-80^{\circ}\text{C}$  temperature until testing within 48 hours. Written consents were obtained from the patients whose samples were positive for SARS-CoV-2 to allow their samples to be further analyzed for publication.

### 2.2. Extracting Viral RNA from Infected Cells

The test was designed to detect the viral RNA in the infected cells as well as in cell-free fluid. To this end, about 1 mL of the nasopharyngeal swab rinse was transferred to a graduated 1.5 mL microcentrifuge tube and centrifuged at  $\sim 16,000\times g$  for 5 min to pellet all cells and cellular debris. The supernatant was discarded except for the last 0.2 mL, which was left in the test tube with the pellet. To each test tube containing the pellet and the residual fluid, 200  $\mu\text{L}$  of digestion buffer containing 1% sodium dodecyl sulfate, 20 mM Tris-HCl (pH 7.6), 0.2M NaCl and 700  $\mu\text{g}/\text{mL}$  proteinase K, was added. The mixture was digested at  $47^{\circ}\text{C}$  for 1 hr in a shaker. An equal volume (400  $\mu\text{L}$ ) of acidified 125:24:1 phenol:chloroform:isoamyl alcohol mixture (Thermo Fisher Scientific Inc.) was added to each tube. After vortexing for extraction and centrifugation at  $\sim 16,000\times g$  for 5 min to separate the phases, the phenol extract was aspirated out and discarded. Another volume of 300  $\mu\text{L}$  of acidified 125:24:1 phenol:chloroform:isoamyl alcohol mixture was added to the aqueous solution for a second extraction. After centrifugation at  $\sim 16,000\times g$  for 5 min to separate the phases, 200  $\mu\text{L}$  of the aqueous supernatant without any material at the interface was transferred to a new 1.5 mL microcentrifuge tube. To the 200  $\mu\text{L}$  aqueous sample, 20  $\mu\text{L}$  of 3M sodium acetate (pH5.2) and 570  $\mu\text{L}$  of 95% ethanol were added. The mixture was placed in a cold metal block in a freezer set at  $-15$  to  $-20^{\circ}\text{C}$  for 20 min, and then centrifuged at  $\sim 16,000\times g$  for 5 min. The precipitated nucleic acid was washed

with 700  $\mu\text{L}$  of cold 70% ethanol. After a final centrifugation at  $\sim 16,000\times g$ , the 70% ethanol was completely removed with a fine-tip pipette, and the microcentrifuge tube with opened cap was put into a vacuum chamber for 10 minutes to evaporate the residual ethanol. The nucleic acids in each tube were dissolved in 50  $\mu\text{L}$  of diethylpyrocarbonate treated water (ThermoFisher). All nucleic acid extracts were tested immediately or stored at  $-80^\circ\text{C}$  until testing.

### 2.3. PCR Conditions

To initiate the primary RT-PCR, a total volume of 25  $\mu\text{L}$  mixture was made in a PCR tube containing 20  $\mu\text{L}$  of ready-to-use LoTemp<sup>®</sup> PCR mix with denaturing chemicals (HiFi DNA Tech, LLC, Trumbull, CT, USA), 1  $\mu\text{L}$  (200 units) of Invitrogen SuperScript III Reverse Transcriptase, 1  $\mu\text{L}$  (40 units) of Ambion<sup>™</sup> RNase Inhibitor, 0.1  $\mu\text{L}$  of Invitrogen 1 M DTT (dithiothreitol), 1  $\mu\text{L}$  of 10  $\mu\text{M}$  forward primer in TE buffer, 1  $\mu\text{L}$  of 10  $\mu\text{M}$  reverse primer in TE buffer and 1  $\mu\text{L}$  of sample nucleic acid extract. The ramp rate of the thermal cycler was set to  $0.9^\circ\text{C}/\text{s}$ . The program for the temperature steps was set as:  $47^\circ\text{C}$  for 30 min to generate the cDNA,  $85^\circ\text{C}$  1 cycle for 10 min, followed by 30 cycles of  $85^\circ\text{C}$  30 sec for denaturing,  $50^\circ\text{C}$  30 sec for annealing,  $65^\circ\text{C}$  1 min for primer extension, and final extension  $65^\circ\text{C}$  for 10 minutes. The nested PCR was conducted in a 25  $\mu\text{L}$  volume of complete PCR mixture containing 20  $\mu\text{L}$  of ready-to-use LoTemp<sup>®</sup> PCR mix, 1  $\mu\text{L}$  of 10  $\mu\text{M}$  forward primer, 1  $\mu\text{L}$  of 10  $\mu\text{M}$  reverse primer and 3  $\mu\text{L}$  of molecular grade water. To initiate the nested PCR, a trace (about 0.2  $\mu\text{L}$ ) of primary PCR products was transferred by a micro-glass rod to the complete nested PCR mixture. The thermocycling steps were programmed to  $85^\circ\text{C}$  1 cycle for 10 min, followed by 30 cycles of  $85^\circ\text{C}$  30 sec for denaturing,  $50^\circ\text{C}$  30 sec for annealing,  $65^\circ\text{C}$  1 min for primer extension, and final extension  $65^\circ\text{C}$  for 10 minutes. Transferring of PCR products was carried out by micro-glass rods in a PCR station, not by micropipetting, to avoid aerosol contamination.

### 2.4. DNA Sequencing

The crude nested PCR products showing an expected amplicon at agarose gel electrophoresis were subjected to automated Sanger sequencing without further purification. To initiate the Sanger reaction, a trace (about 0.2  $\mu\text{L}$ ) of nested PCR products was transferred by a micro-glass rod into a thin-walled PCR tube containing 1  $\mu\text{L}$  of 10  $\mu\text{M}$  sequencing primer, 1  $\mu\text{L}$  of BigDye<sup>®</sup> Terminator (v 1.1/Sequencing Standard Kit), 3.5  $\mu\text{L}$   $5\times$  buffer, and 14.5  $\mu\text{L}$  water in a total volume of 20  $\mu\text{L}$ . Twenty (20) enzymatic primer extension/termination reaction cycles were run according to the protocol supplied by the manufacturer (Applied Biosystems, Foster City, CA, USA). After a dye-terminator cleanup, the Sanger reaction mixture was loaded in an Applied Biosystems SeqStudio Genetic Analyzer for sequence analysis. Sequence alignments were performed against the standard sequences stored in the GenBank database by online

BLAST. The sequences were also visually analyzed for nucleotide mutations and indels.

## 2.5. PCR Primers

The sequences of the primary and nested PCR primers used in this study for amplification of the N gene and the RBD are summarized in **Table 1**.

## 2.6. Summary of Workflow

The workflow from nucleic acid extraction to variant determination by Sanger sequencing is summarized in **Figure 1**.

**Table 1.** Primary and nested PCR primers and their sequences were used in this study.

PCR Amplicon	Primer Type	Start	End	Sequence 5'-3'	Size (bp)
SARS-CoV-2 N gene Co4/Co3 Nested	Co1 primary F.	28,707	28,727	ACATTGGCACCCGCAATCCTG	416
	Co8 primary R.	29,102	29,122	TTGGGTTTGTCTGGACCACG	
	Co4 nested F.	28,720	28,740	CAATCCTGCTAACAATGCTGC	<u>398</u>
	Co3 nested R.	29,097	29,117	TTTGTCTGGACCACGTCCTGC	
SARS-CoV 2 S gene RBD S9/S10 Nested	SS1 primary F.	22,643	22,663	TGTGTTGCTGATTATTCGTGTC	460
	SS2 primary R.	23,082	23,102	AAAGTACTACTACTCTGTATG	
	S9 nested F.	22,652	22,672	GATTATTCTGTCCTATATAAT	<u>445</u>
	S10 nested R.	23,076	23,096	CTACTACTCTGTATGGTTGGT	

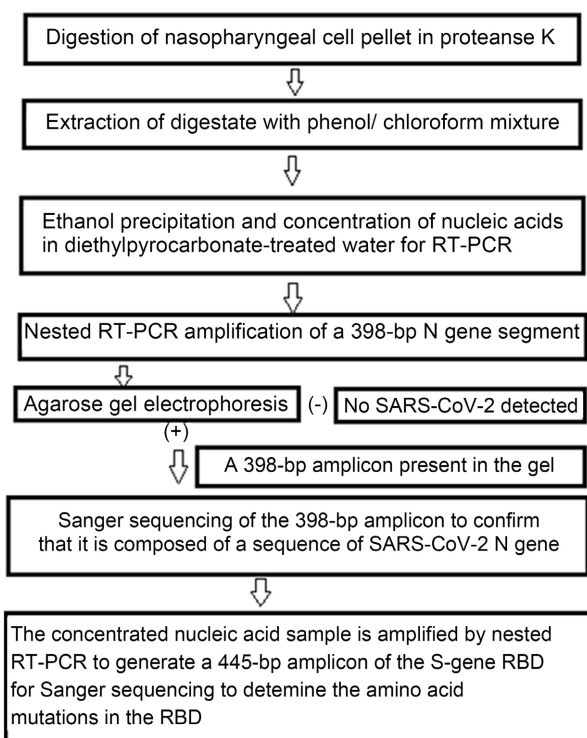


**Figure 1.** Workflow diagram for SARS-CoV-2 detection and variant determination by Sanger sequencing.

### 3. Results

#### 3.1. SARS-CoV-2 Omicron BA.2.86 (+JN.1) N Gene Sequence (Figure 2)

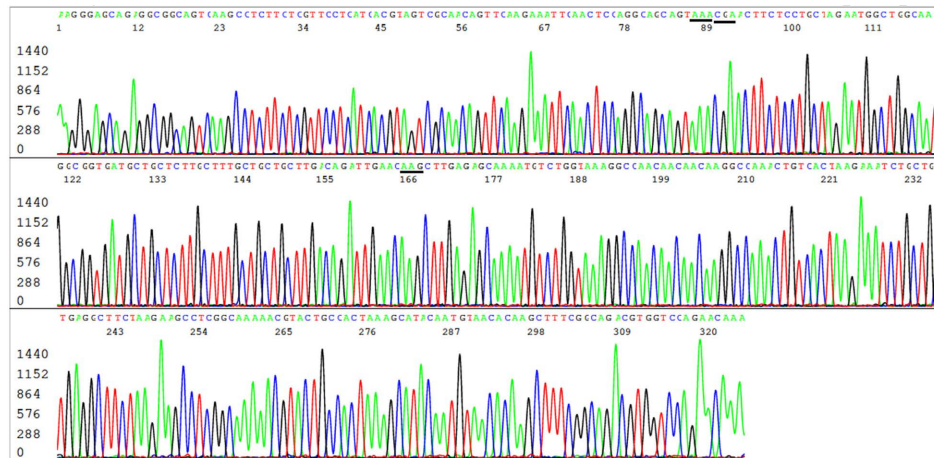


**Figure 2.** Electropherogram showing an N gene forward sequence of SARS-CoV-2 Omicron JN.1 variant. The reverse Co3 primer is in the end of the sequence. The codons of the 3 amino acid mutations, R203K (AGG > AAA), G204R (GGA > CGA) and Q229K (CAG > AAG), usually associated with BA.2.86 (+JN.1) are underlined. An N-gene sequencing cannot distinguish JN.1 variant from its predecessor Omicron BA.2.86.

#### 3.2. SARS-CoV-2 Omicron JN.1 S-Gene RBD Sequence

##### 3.2.1. S-Gene RBD forward Sequencing (Figure 3)

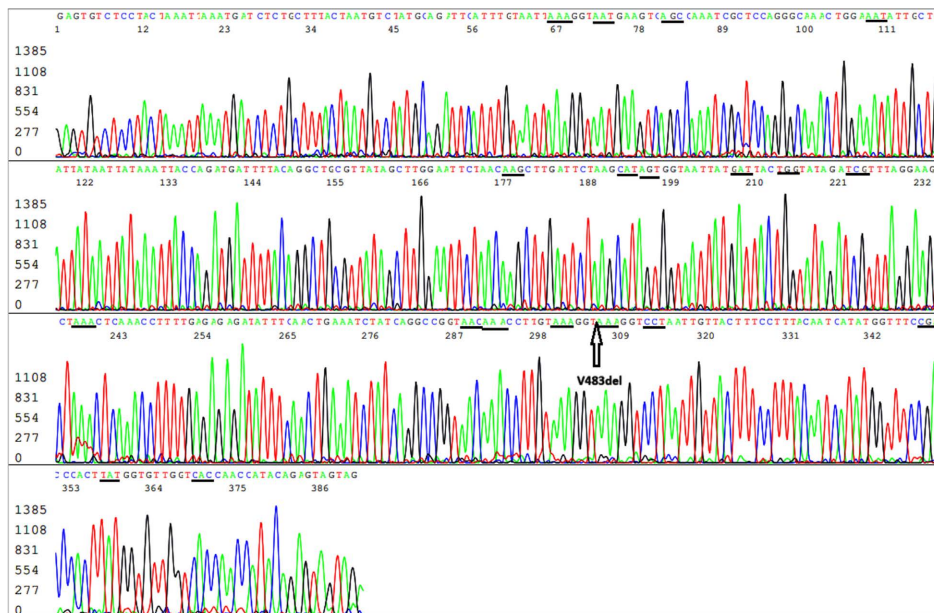


**Figure 3.** Electropherogram showing an S-gene RBD forward sequence of SARS-CoV-2 Omicron JN.1 variant. The S10 reverse nested PCR primer is in the end of the sequence. The codons of the 19 amino acid mutations included in this sequence, namely R403K (AGA > AAA), D405N (GAT > AAT), R408S (AGA > AGC), K417N (AAG > AAT), N440K (AAT > AAG), V445H (GTT > CAT), G446S (GGT > AGT), N450D (AAT > GAT), L452W (CTG > TGG), L455S (TTG > TCG), N460K (AAT > AAA), S477N (AGC > AAC), T478K (ACA > AAA), N481K (AAT > AAA), E484K (GAA > AAA), F486P (TTT > CCT), Q498R (CAA > CGA), N501Y (AAT > TAT) and Y505H (TAC > CAC), are underlined. The position of V483del is pointed by an arrow. The L455S mutation in the RBD distinguishes JN.1 variant from its predecessor Omicron BA.2.86.

### 3.2.2. S-Genes RBD Reverse Sequencing (Figure 4)

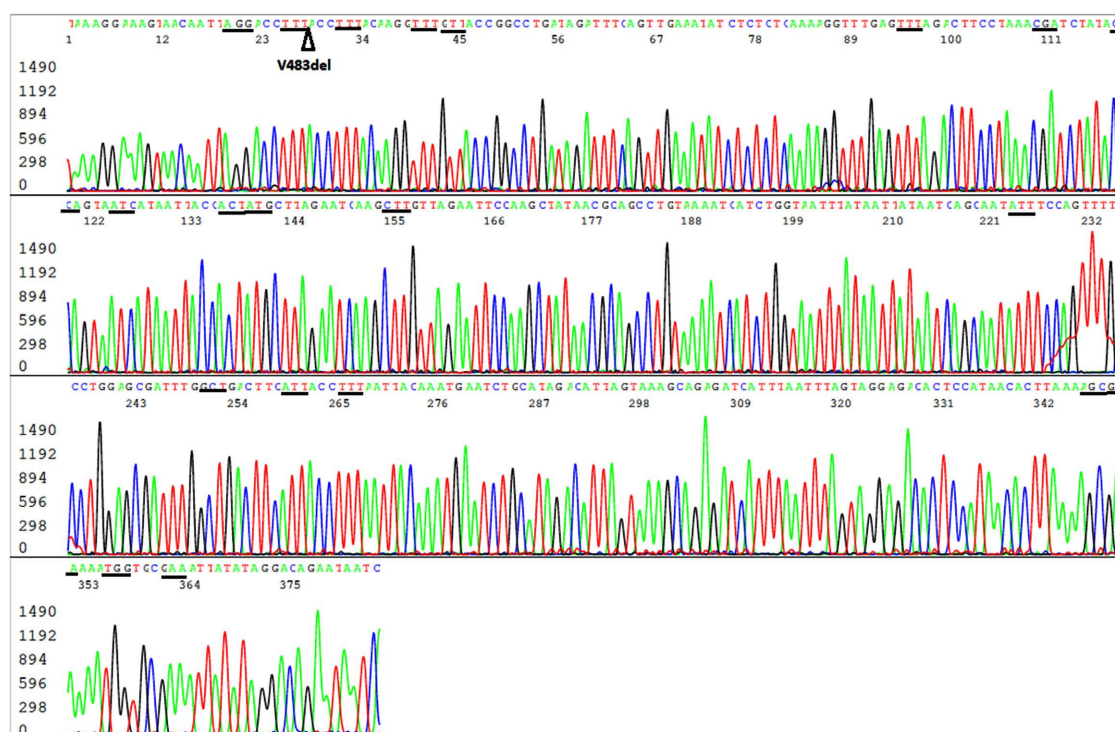


**Figure 4.** Electropherogram showing an S-gene RBD reverse sequence of SARS-CoV-2 Omicron JN.1 variant. The S9 forward nested PCR primer is in the end of the sequence. The codons (in reverse complement) of the 20 amino acid mutations included in this sequence, namely F486P, E484K, N481K, T478K, S477N, N460K, L455S, L452W, N450D, G446S, V445H, N440K, K417N, R408S, D405N, R403K, T376A, S375F, S373P and S371F, are underlined. The position of V483del is pointed by an arrowhead.

## 4. Discussion

The results presented in this paper confirm that implementation of routine sequencing of a 445-bp RT-PCR amplicon of the SARS-CoV-2 S-gene in CLIA-certified diagnostic laboratories can identify almost all the amino acid mutations in the RBD for accurate determination of SARS-CoV-2 variants [10], including the latest dominant JN.1 variant by demonstrating its hallmark L455S mutation (Figure 3 and Figure 4). Sequencing a 398-bp segment of the N-gene for molecular diagnosis of SARS-CoV-2 can confirm the Omicron BA.2.82 (+LN.1) lineage because there is a unique Q229K mutation in this lineage (Figure 2) but cannot verify JN.1. However, targeting the N-gene for SARS-CoV-2 RT-PCR generates less primer failures because the N-gene mutates less frequently than the S-gene [10].

The value of Sanger sequencing of the S-gene and RBD for accurate determination of SARS-CoV-2 variants has been recognized by other investigators. For example, Rodrigues and colleagues amplified a 1006 bp fragment of the S-gene, including the RBD, for variant determination in specimens with an RT-qPCR Ct values  $\leq 20$  [11]. Bloemen and colleagues amplified a 733-bp segment of the S gene and sent the purified PCR products to a commercial company for Sanger sequencing [12]. But for clinical diagnostic work where complex human speci-

mens are involved, the size of the PCR amplicons should be <500 bp to avoid loss of PCR sensitivity [13]. As shown in **Figure 3** and **Figure 4**, bidirectional sequencing of a 445-bp fragment of the RBD covers all amino acid mutations from S371F to Y505H, the key mutations that are commonly used for accurate variant determination.

The CDC's relying on using TaqPath COVID-19 Combo Kit (Thermo Fisher Scientific) as the method to define JN.1 or non-JN.1 infections for statistical analysis to support the claim of effectiveness of updated monovalent XBB.1.5 COVID-19 vaccines against symptomatic infection with the JN.1 lineage [7] is questionable. In a convoluted statement "*SARS-CoV-2-positive specimens with either null or reduced amplification of the S-gene (Ct for S-gene > 4 cycles from the average of N and ORF1ab Ct values) were considered to have SGTF, an indication of a particular deletion in the SARS-CoV-2 spike protein, which currently indicates an infection with BA.2.86, JN.1, and their sublineages*" published in its report [7], the CDC has admitted that the TaqPath COVID-19 Combo Kit cannot distinguish between BA.2.86 and JN.1. The rationale for using SGTF as the proxy indicator of JN.1 was based on CDC's National SARS-CoV-2 Strain Surveillance (NS3) program, which shows a very high JN.1/BA.2.86 proportion [2] so that the possibility of detecting a BA.2.86 could be disregarded. However, the CDC's SARS-CoV-2 genomic surveillance relies on using next generation sequencing technologies that require samples containing high viral loads (RT-qPCR Ct values  $\leq 28$ ) to generate quality sequences [14]. As a result, all positive specimens submitted to the National SARS-CoV-2 Strain Surveillance (NS3) program for sequencing have RT-qPCR Ct values  $\leq 28$  [15]. But in real medical practice, most specimens testing positive for SARS-CoV-2 RT-qPCR have a Ct value higher than 27, false positives included [16]. In one comparative study, among 29 true SARS-CoV-2-positive specimens confirmed by Sanger sequencing, 13 of the 29 (~45%) had an RT-qPCR Ct > 28 [10]. In other words, about 45% of the specimens positive for a variant of SARS-CoV-2 are not being sequenced in the national genomic surveillance program because the viral loads in these specimens were not high enough for next generation sequencing, and these patient specimens with low viral loads may contain a non-JN.1 variant that is not included in the current COVID Data Tracker. The very high JN.1 percentage listed in the National SARS-CoV-2 Strain Surveillance may be the result of sample selection bias that cannot be extrapolated to using SGTF as the proxy indicator of JN.1 by statistic exclusion of other possible variants found in routine RT-qPCR testing.

To justify using SGTF as the proxy indicator of JN.1 for statistical analysis, the CDC may consider Sanger-sequencing the S-gene RBD of 500 specimens tested positive by TaqPath COVID-19 Combo Kit regardless RT-qPCR Ct values, 250 with SGTF and 250 with SGTP, to prove that SGTF and SGTP are in fact the appropriate proxy indicators of the presence and absence of L455S, the hallmark mutation of JN.1. The cost for such a small project would be less than \$100,000 that should be well within the CDC budget.



## Funding

No funding was obtained for this study.

## Declaration of Competing Interest

Sin Hang Lee is the director of the Milford Molecular Diagnostics Laboratory specialized in developing DNA sequencing-based diagnostic tests implementable in community hospital laboratories.

## Conflicts of Interest

The author declares no conflicts of interest regarding the publication of this paper.

## References

- [1] ViralZone (2024) Sars-CoV-2 Circulating Variants. <https://viralzone.expasy.org/9556>
- [2] Centers for Disease Control and Prevention (CDC) (2024) Covid Data Tracker. <https://covid.cdc.gov/covid-data-tracker/#variant-proportions>
- [3] Centers for Disease Control and Prevention (CDC) (2023) Update on SARS-CoV-2 Variant JN.1 Being Tracked by CDC. [https://www.cdc.gov/ncird/whats-new/SARS-CoV-2-variant-JN.1.html?CDC\\_AA\\_r ef- Val=https%3A%2F%2Fwww.cdc.gov%2Frespiratory-viruses%2Fwhats-new%2FSA RS-CoV-2-variant-JN.1.html](https://www.cdc.gov/ncird/whats-new/SARS-CoV-2-variant-JN.1.html?CDC_AA_r ef- Val=https%3A%2F%2Fwww.cdc.gov%2Frespiratory-viruses%2Fwhats-new%2FSA RS-CoV-2-variant-JN.1.html)
- [4] Jeworowski, L.M., Mühlemann, B., Walper, F., *et al.* (2024) Humoral Immune Escape by Current SARS-CoV-2 Variants BA.2.86 and JN.1, December 2023. *Euro-surveillance*, **29**, Article ID: 2300740. <https://doi.org/10.2807/1560-7917.ES.2024.29.2.2300740>
- [5] Kaku, Y., Okumura, K., Padilla-Blanco, M., *et al.* (2024) Virological Characteristics of the SARS-CoV-2 JN.1 Variant. *The Lancet Infectious Diseases*, **24**, e82. <https://pubmed.ncbi.nlm.nih.gov/38184005/> [https://doi.org/10.1016/S1473-3099\(23\)00813-7](https://doi.org/10.1016/S1473-3099(23)00813-7)
- [6] Yang, S., Yu, Y., Xu, Y., *et al.* (2024) Fast Evolution of SARS-CoV-2 BA.2.86 to JN.1 under Heavy Immune Pressure. *The Lancet Infectious Diseases*, **24**, e70-e72. [https://doi.org/10.1016/S1473-3099\(23\)00744-2](https://doi.org/10.1016/S1473-3099(23)00744-2) <https://pubmed.ncbi.nlm.nih.gov/38109919/>
- [7] Link-Gelles, R., Ciesla, A.A., Mak, J., *et al.* (2024) Early Estimates of Updated 2023-2024 (Monovalent XBB.1.5) COVID-19 Vaccine Effectiveness against Symptomatic SARS-CoV-2 Infection Attributable to Co-Circulating Omicron Variants Among Immunocompetent Adults—Increasing Community Access to Testing Program, United States, September 2023-January 2024. *Morbidity and Mortality Weekly Report (MMWR)*, **73**, 77-83. <https://pubmed.ncbi.nlm.nih.gov/38300853/> <https://doi.org/10.15585/mmwr.mm7304a2>
- [8] Guerra-Assunção, J.A., Boshier, F.A.T., Crone, M.A., *et al.* (2021) Reliability of Spike Gene Target Failure for ascertaining SARSCoV-2 Lineage B.1.1.7 Prevalence in a Hospital Setting. Preprint. <https://doi.org/10.1101/2021.04.12.21255084>
- [9] Lee, S.H. (2021) A Routine Sanger Sequencing Target Specific Mutation Assay for

- SARS-CoV-2 Variants of Concern and Interest. *Viruses*, **13**, Article 2386.  
<https://www.ncbi.nlm.nih.gov/pmc/articles/PMC8706074/>  
<https://doi.org/10.3390/v13122386>
- [10] Lee, S.H. (2022) Evidence-Based Evaluation of PCR Diagnostics for SARS-CoV-2 and the Omicron Variants by Gold Standard Sanger Sequencing. *Science, Public Health Policy, and the Law*, **4**, 144-189.  
[https://www.publichealthpolicyjournal.com/files/ugd/adf864\\_01b8d2e159014d53a342e807a540c143.pdf](https://www.publichealthpolicyjournal.com/files/ugd/adf864_01b8d2e159014d53a342e807a540c143.pdf)  
<https://doi.org/10.20944/preprints202204.0091.v1>
- [11] Rodrigues, G.M., Volpato, F.C.Z., Wink, P.L., Paiva, R.M., Barth, A.L. and de-Paris, F. (2023) SARS-CoV-2 Variants of Concern: Presumptive Identification via Sanger Sequencing Analysis of the Receptor Binding Domain (RBD) Region of the S Gene. *Diagnostics (Basel, Switzerland)*, **13**, Article 1256.  
<https://doi.org/10.3390/diagnostics13071256>
- [12] Bloemen, M., Rector, A., Swinnen, J., Ranst, M.V., Maes, P., Vanmechelen, B. and Wollants, E. (2022) Fast Detection of SARS-CoV-2 Variants Including Omicron Using One-Step RT-PCR and Sanger Sequencing. *Journal of Virological Methods*, **304**, Article ID: 114512. <https://doi.org/10.1016/j.jviromet.2022.114512>
- [13] McCarty, S.C. and Atlas, R.M. (1993) Effect of Amplicon Size on PCR Detection of Bacteria Exposed to Chlorine. *PCR Methods and Applications*, **3**, 181-185.  
<https://doi.org/10.1101/gr.3.3.181>
- [14] Goswami, C., Sheldon, M., Bixby, C., *et al.* (2022) Identification of SARS-CoV-2 Variants Using Viral Sequencing for the Centers for Disease Control and Prevention Genomic Surveillance Program. *BMC Infectious Diseases*, **22**, Article No. 404.  
<https://doi.org/10.1186/s12879-022-07374-7>  
<https://pubmed.ncbi.nlm.nih.gov/35468749/>
- [15] Updated CDC Guidance for Specimen Submission for Surveillance of SARS-CoV-2 (NS3).  
[https://www.aphl.org/programs/infectious\\_disease/Documents/NS3%20Guidance%20with%20Appendix%201%20.pdf](https://www.aphl.org/programs/infectious_disease/Documents/NS3%20Guidance%20with%20Appendix%201%20.pdf)
- [16] Tartof, S.Y., Slezak, J.M., Fischer, H., *et al.* (2021) Effectiveness of mRNA BNT162b2 COVID-19 Vaccine up to 6 Months in a Large Integrated Health System in the USA: A Retrospective Cohort Study. *Lancet*, **398**, 1407-1416.  
<https://pubmed.ncbi.nlm.nih.gov/34619098/>  
[https://doi.org/10.1016/S0140-6736\(21\)02183-8](https://doi.org/10.1016/S0140-6736(21)02183-8)